ELSEVIER

Spectrochimica Acta Part B 51 (1996) 1473–1485

SPECTROCHIMICA ACTA PART B

Laser ablation solid sampling: vertical spatial emission intensity profiles in inductively coupled plasma

Manuel Caetano[b], Xianglei Mao[a], Richard E. Russo[a,*]

[a]*Lawrence Berkeley National Laboratory, Berkeley, CA 94720, USA*
[b]*Escuela de Química, Universidad Central de Venezuela, Caracas 1041-A, Venezuela*

Received 23 January 1996; accepted 26 April 1996

Abstract

Spectral emission intensity in the inductively coupled plasma (ICP) was measured versus height above the load coil during laser ablation solid-sample introduction. The laser-beam pulse width, power density, and wavelength, and the sample composition are know to effect the particle size distribution of the ablated mass. Ceramic and metal samples were ablated using nanosecond and picosecond pulses, and provided similar emission intensity profiles for common elements, indicating that changes in the particle size distribution are not manifested in the vertical spatial emission profile. The gas environment in the ablation chamber also influences the particle size distribution as well as the ablation interaction. Gas composition will influence the spatial emission intensity profile because of changes in the excitation characteristics of the ICP. A preliminary study using noble gases in the ablation interaction was conducted by keeping the spatial profile constant, maintaining a constant total gas composition to the ICP.

Keywords: Atomic emission spectroscopy; Inductively coupled plasma; Laser ablation; Noble gases; Solid sampling; Vertical spatial emission intensity profile

1. Introduction

Laser ablation (LA) with inductively-coupled plasma atomic emission spectroscopy (ICP-AES) offers numerous advantages for direct solid-sample chemical analysis [1–9]. ICP-AES is also a viable technology for studying laser ablation processes at atmospheric pressure [1,9–13]. Spectral emission intensity in the ICP is related to the quantity of mass ablated, which exhibits a non-linear dependence on laser power density [1,9,10,12,14]. A potential cause of this non-linear dependence could be a change in the ablated particle size distribution. The ablated particle size distribution depends on the laser-beam parameters (pulse duration, wavelength, and fluence), ambient gas and pressure, and physical properties of the solid sample [15–19]. A wide range of power densities are employed in laser ablation solid sampling, depending on the laser and its operating properties (Q-switch versus normal) with higher values generally accepted to minimize preferential vaporization [9,11,14,20,21]. The vertical spatial distribution of the analyte in the ICP may be influenced by particle size changes. Although the spatial emission profile will be governed primarily by the ICP power and gas flow characteristics, different sized particles can influence the temperature characteristics of the plasma spatially. Analytical accuracy and sensitivity

* Corresponding author.

PII S0584-8547(96)01539-X

would be compromised because of a change in the optimum observation height above the load coil for atomic emission spectroscopy, or sampling location of the orifice for mass spectrometry.

The sample chamber gas environment can influence the particle size distribution, as well as fundamental processes such as plasma shielding [10,15,16]. Gas composition will influence the spatial emission intensity profile because of changes in the excitation characteristics of the ICP. To study fundamental ablation processes versus gases using ICP-AES, it is necessary to maintain a constant spatial emission intensity profile.

Of course, spatial emission profile behavior for different laser conditions or sample properties does not directly describe ablation sampling processes, because transport will bias these data [18,19,22,23]. Transport allows only a fixed particle size distribution to reach the ICP, so that even if the distribution changes, the ICP primarily responds to the change in the number of particles within that distribution. In Arrowsmith's model, transport efficiency dropped significantly for particles greater than approximately 3 μm [18]. Particle collection studies showed that only a small number of larger particles (5–12 μm) were produced by laser ablation, although they contained a significant fraction of the ablated mass [18,19,22]. van Heuzen showed that particles were produced from glass beads up to 30 μm in diameter although only those less than about 10 μm were entrained, and only the 0.5–3 μm particles were transported into the ICP [22,23]. In addition, large particles may not be completely vaporized in the ICP. From slurry ICP studies, only particles < 3 μm reside sufficiently long in the ICP [24–28] for vaporization and atomization. It is important to point out that the particle size distribution generated and transported to the ICP is governed by the design of the particular experimental system. All published results are for specific lasers, chambers, and flow configurations; particle size distribution and transport are not expected to be the same for every laboratory.

The goal of this work was to induce a significant change in the particle size distribution and determine any influence on the spatial emission intensity profile in the ICP. Ablation was performed using diverse laser parameters (power density, pulse width, and wavelength), metal and ceramic samples, and noble gases in the ablation chamber. A CCD spectrometer was used to monitor several wavelengths simultaneously, and to monitor the vertical spatial emission profile in the ICP during laser ablation solid-sample introduction under these various conditions.

2. Experimental

A diagram of the experimental system is shown in Fig. 1. Two different lasers were used for ablation: a KrF excimer laser with λ = 248 nm, and a Nd:YAG with λ = 266 nm and 1064 nm. The pulse duration of the excimer and Nd:YAG were 30 ns and 35 ps, respectively. Each laser was pulsed at a repetition rate of 10 Hz. Both laser beams were apertured using a 6 mm diameter iris, and focused into the sample chamber using a plano-convex UV grade quartz lens (f = 200 nm). The lens was mounted on a micrometer translation stage in order to accurately adjust the laser-beam spot size at the sample surface. A quartz sample chamber was fixed on an xyz micrometer translation stage so the ablated area could be changed after each measurement. The quartz chamber was 30 mm in diameter and 80 mm in length with 6 mm diameter gas ports. The gas inlet and outlet ports were 2 mm and 10 mm beyond the sample, respectively. The laser power density was controlled by fixing the laser energy and varying the lens to target distance; the spot size of the laser beam on the target surface was changed. Power density at the sample surface was calculated from the energy of the laser beam, the pulse width, and the spot area. The spot area was estimated using geometric optical principles and compared to burn pattern measurements.

The samples consisted of small discs (2 cm diameter and 1 mm thickness) of metallic brass, Cu, Al, and the ceramic Al_2O_3. The flow of gases to the ablation chamber and ICP was regulated using mass flow controllers (Matheson; 8274). The exit port of the ablation chamber was connected to a steel T-coupler (Swagelock), so that the carrier gas could be combined with an auxiliary gas and the resultant mixture introduced to the central channel of the ICP torch. Both flows were 0.50 l min^{-1}; the flow in the central channel of the ICP was 1.0 l min^{-1}. This mixing procedure ensures that the ICP conditions are constant when studying laser ablation versus different gas

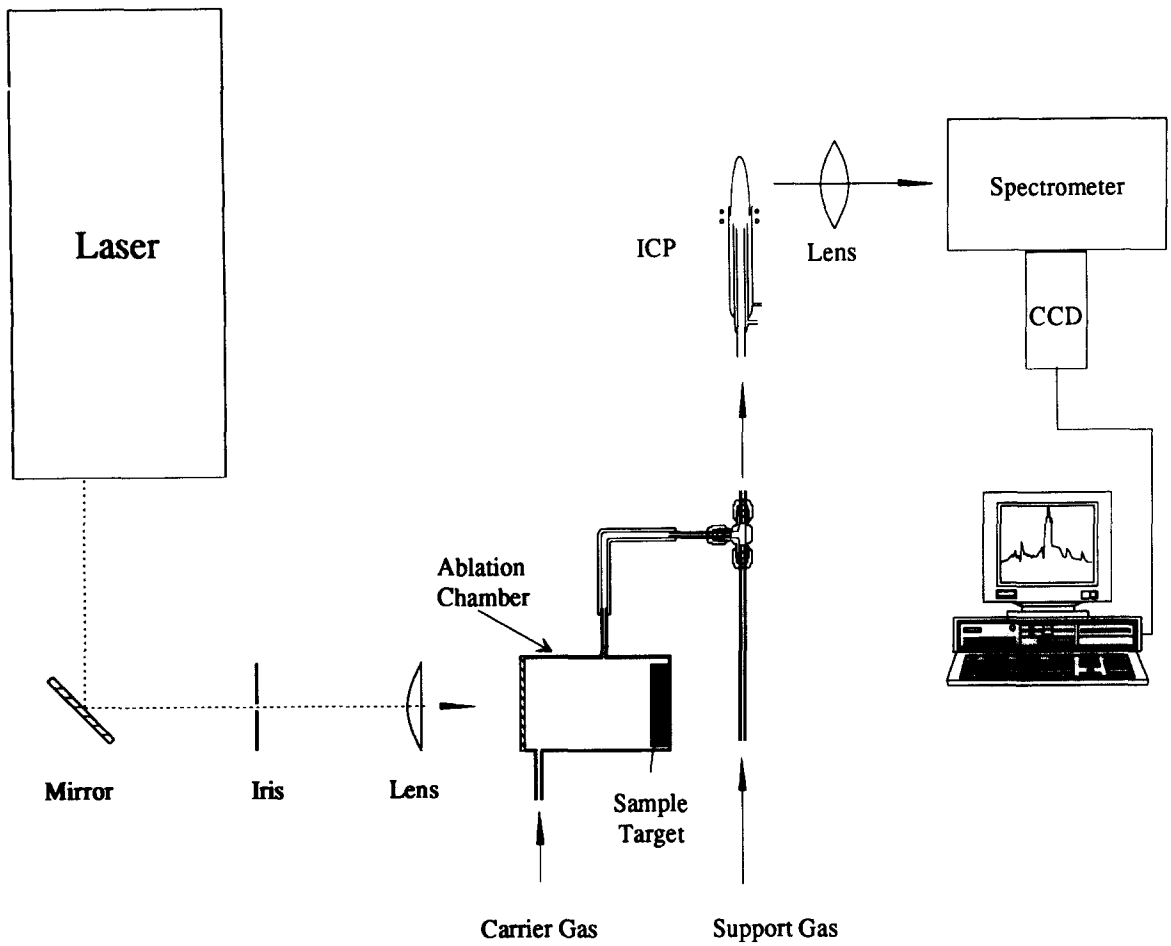

Fig. 1. Diagram of the experimental laser ablation sampling ICP-AES system with CCD detector for measuring emission spatial profiles.

environments. The ICP (Plasma Therm; 2500D, 27 MHz) was operated at 1.25 kW forward power and 14.0 l min^{-1} outer Ar gas flow. The reflected power was maintained below 1 W. The ICP conditions affect the observed emission intensities [29]; for these studies, the RF power and the gas flow rates are kept constant. A separate investigation of ICP power and gas flow conditions for laser ablation sampling has been conducted [30].

Spectral emission from the ICP was imaged using a quartz lens (5 cm focal length) onto a 0.27 m monochromator (Spex industries; 270M) with a 1200 grooves mm^{-1} holographic grating and a slit width of 25 μm. The detector was a Peltier cooled CCD with 512 × 512 pixels (EG and G PAR; OMA VISION). This spectrometer system simultaneously measures a 30 nm wavelength range, with a spectral resolution of 0.059 nm defined by the pixels of the CCD. The imaged region was centered on the analyte channel of the ICP from below the load coil to approximately 40 mm above. Data from the CCD were digitized and transferred to a microcomputer.

Spectral emission intensities are integrated during repetitive ablation/sampling, after a 120 s pre-ablation. Pre-ablation and repetitive pulsing at the same sample location stabilize the laser ablation process and improve precision [1,9,11,14,31,32]. The emission intensity was corrected by subtracting the ICP background emission, measured in the absence of ablation sampling. The wavelength range monitored for brass and copper samples was 200–230 nm. For brass, Cu(II) emission lines at 224 nm and the Zn(I)

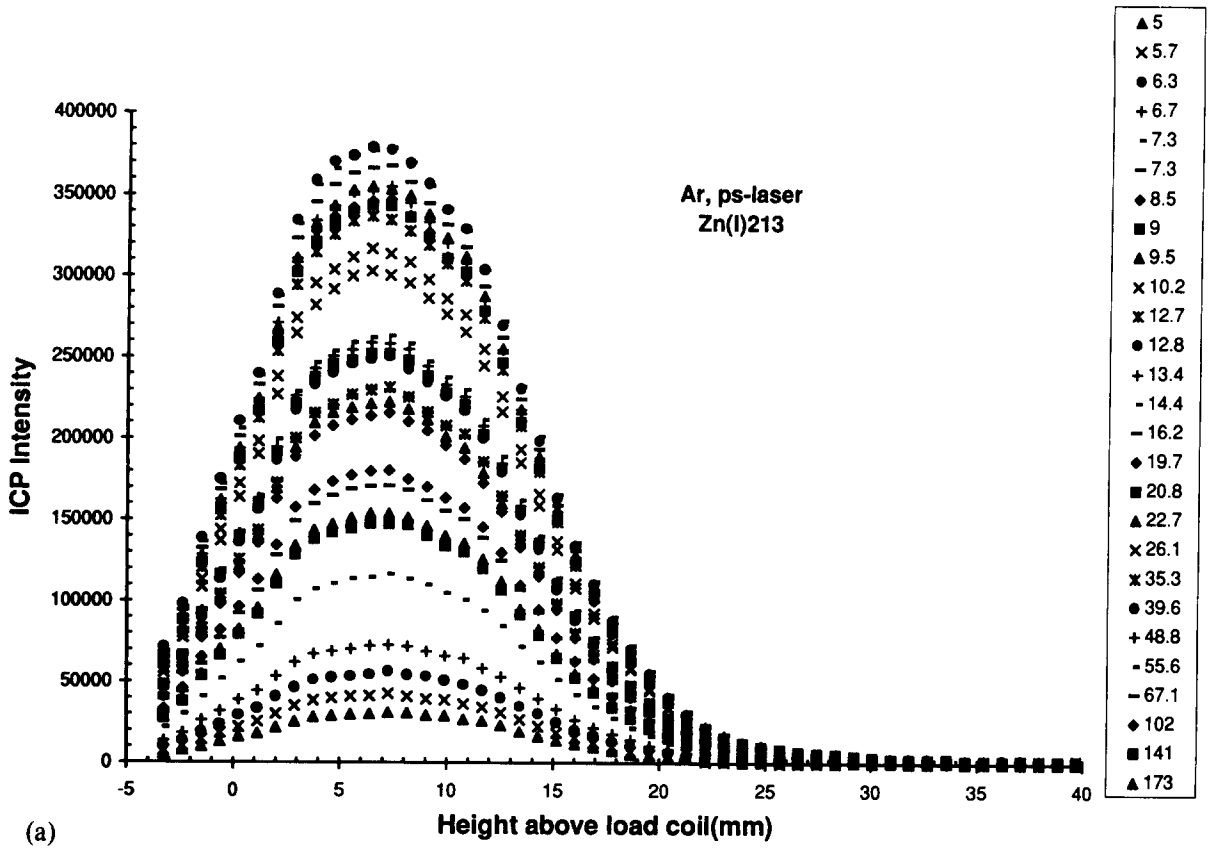

Fig. 2. Zinc emission intensity in the ICP using picosecond laser ablation sampling of brass. (a) emission intensity versus height above the load coil at each power density; (b) normalized emission intensity for all power densities; (c) integrated emission intensity versus power density showing the roll-off.

emission line 213 nm could be monitored simultaneously. For aluminum and the insulator Al_2O_3, the CCD spectrometer range was 295–325 nm.

3. Results and discussion

3.1. Spatial emission profiles versus laser properties

The plateau and roll-off in ICP emission intensity with increasing laser power density has been hypothesized as a decrease in the laser–sample interaction efficiency and/or as a significant change in the particle size distribution [1,9,11,13,14,33]. The particle size distribution may influence the vertical spatial distribution of analyte vapor in the ICP, which would be manifested as a shift in the spatial emission intensity profile. To address this possibility, the vertical spatial emission intensity profile in the ICP was measured using diverse laser and sample properties. Zn emission in the ICP as a function of height above the load coil during laser ablation sampling of brass using the picosecond pulsed Nd:YAG laser with power density from approximately 5 to 173 GW cm^{-2} is shown in Fig. 2. Fig. 2a shows the individual intensity profiles for each power density; Fig. 2b shows a constant spatial profile when these data are normalized; and Fig. 2c shows the integrated peak intensity normalized to beam area versus power density, demonstrating the roll-off. The intensity changes as the laser power density is increased, but the position of the peak and the profile shape remain the same. The emission spatial profiles of Cu exhibited behavior similar to those of Zn. In agreement with previous measurements, the

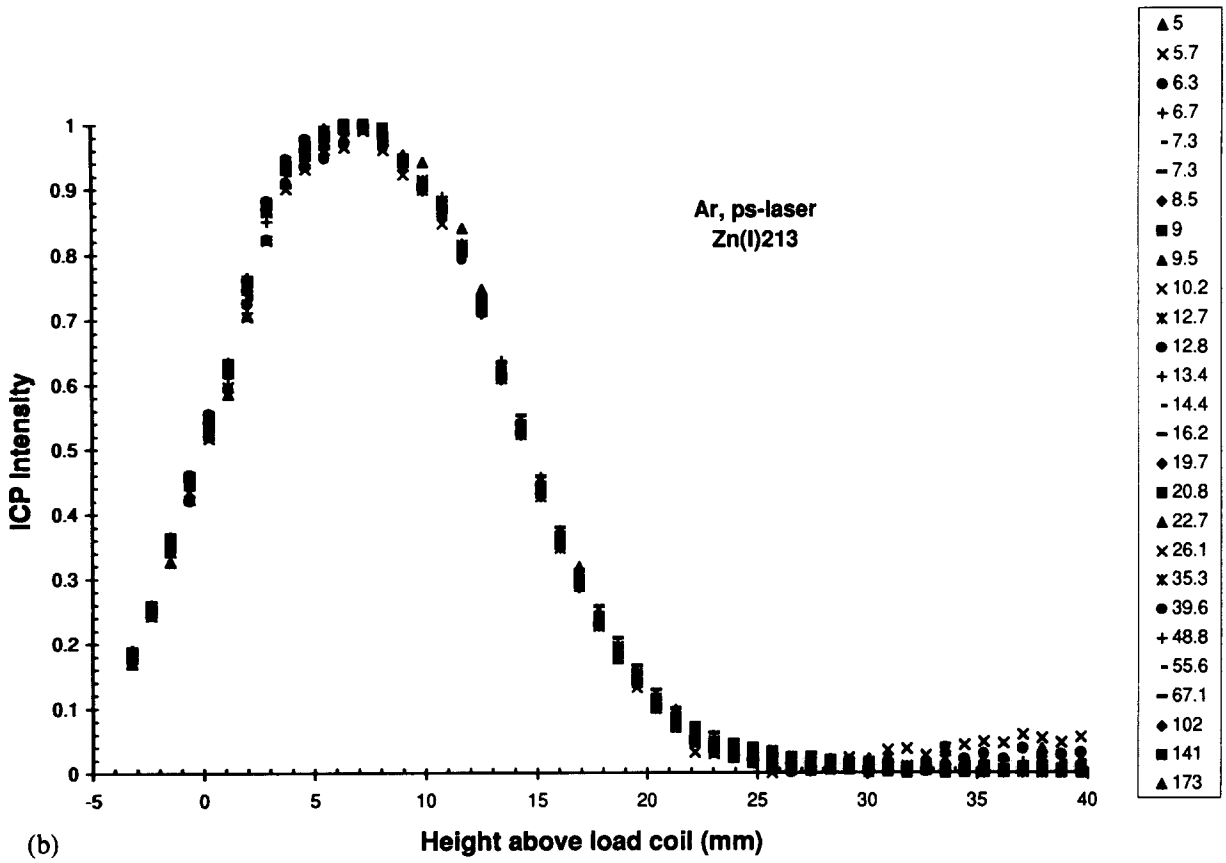
Ar, ps-laser
Zn(I)213
ICP Intensity
Height above load coil (mm)
▲5
×5.7
●6.3
+6.7
-7.3
–7.3
◆8.5
■9
▲9.5
×10.2
✱12.7
●12.8
+13.4
-14.4
–16.2
◆19.7
■20.8
▲22.7
×26.1
✱35.3
●39.6
+48.8
-55.6
–67.1
◆102
■141
▲173

(b)

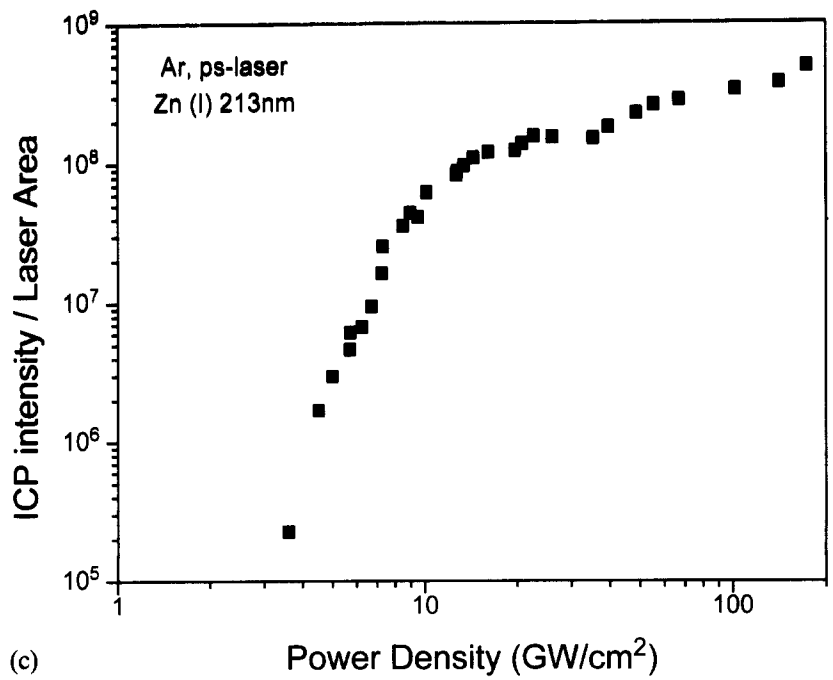
Ar, ps-laser
Zn (I) 213nm
ICP intensity / Laser Area
Power Density (GW/cm²)

(c)

change in the emission intensity (integrated or peak) normalized to beam area, I/A, follows a power-law dependence, $I/A = CP^m$, where I is the ICP emission intensity, A is the laser-beam area, C is constant, P is the power density, and m is the slope indicating the change in log of mass removal versus log of power density (Fig. 2c). The mass removal rate follows two distinct rate behaviors, indicating a change in the laser ablation sampling processes. However, over this wide power density range, the ICP emission spatial profile does not change. Therefore, if the particle size distribution changes significantly, as expected over this broad power density range, either transport selectively filters that portion capable of entrainment, the ICP properties (temperature, ionization) govern the emission profile for the particle size distribution excited in the ICP, or time integration washes out any particle influence on the spatial profile.

Previously, we demonstrated that spectral emission in the ICP consisted of a large number of spikes imposed on a lower continuous level, using repetitively pulsed laser ablation sampling [9]. Liu and Horlick also observed this emission behavior, and proposed monitoring spike emission for enhanced sensitivity [34]. Spike emission is observed when using a photomultiplier tube with fast detection electronics and data acquisition. With time integration, this spike emission is averaged into a slightly higher continuous level. We proposed that the spikes represented larger particles undergoing atomization and excitation during their transport through the ICP. The number of emission spikes was found to be dependent on the laser power density, an indication that the particle size distribution is changing with power density. The number of emission spikes decreased as the laser power density increased. In this work, the CCD detector was used to record the emission spatial profiles. There was no measurable difference in the profile when using either 5 ms or 5 s integration time. 5 ms was the lower limit established by the sensitivity for the elements investigated.

A nanosecond pulsed interaction is expected to provide a different particle distribution than that using picosecond pulses [15–17]. Therefore, the excimer laser was used to ablate the same brass sample using power densities from approximately 0.1 to 6.5 GW cm^{-2} (Fig. 3). Again, the spatial profile remains the same (Fig. 3a), even through the roll-off region (Fig. 3b). The profiles in Figs 2 and 3 cannot be compared because these data were measured several weeks apart using different imaging systems. Data recorded using exact conditions (imaging, gas flow, and ICP conditions) on the same day are shown in Fig. 4. The effect of laser pulse width on the emission spatial profile was studied using the excimer laser (30 ns, λ = 248 nm) versus the fourth harmonic of the Nd:YAG laser (35 ps, λ = 266 nm) (Fig. 4a). Although the laser energy and spot area were very similar, the ICP emission intensity using the 35 ps pulse duration was approximately 10 times greater than that for the 30 ns pulses. The normalized data in Fig. 4b confirm that the ICP spatial emission profile remains constant for these diverse laser ablation conditions. From thin film pulsed laser deposition and other studies, particle size distribution is found to shift to smaller values at lower wavelengths [35–37]. The spatial emission profile remained constant for both UV and IR laser ablation sampling (Fig. 4b). These experimental data, obtained using diverse laser parameters (pulse width, power density, and wavelength), demonstrate that changes in the particle size distribution do not influence the spatial excitation characteristics within the ICP.

3.2. *Spatial emission profiles versus sample properties*

The thermo-optical properties of the sample material will influence the ablated particle morphology and size distribution [14–17,19,22,23]. Ablation from metals and alloys regularly produces smooth molten spherical particles whereas ablation from ceramics and glasses can produce rough, broken, irregularly shaped particles. Such variation in the particle size and morphology might be expected to influence the spatial emission profile in the ICP. However, the measured spatial emission intensity profile was similar for common elements from different samples. The data in Fig. 5 show Al emission versus height above the load coil from ablation of aluminum metal and aluminum oxide ceramic, over a wide power density range using the nanosecond excimer laser. Constant profiles were measured for Cu during ablation of copper and brass targets. As expected, the Al emission profile is different than that from Cu and other elements, owing to temperature and excitation characteristics of the ICP [29]. The spatial distribution remained constant for

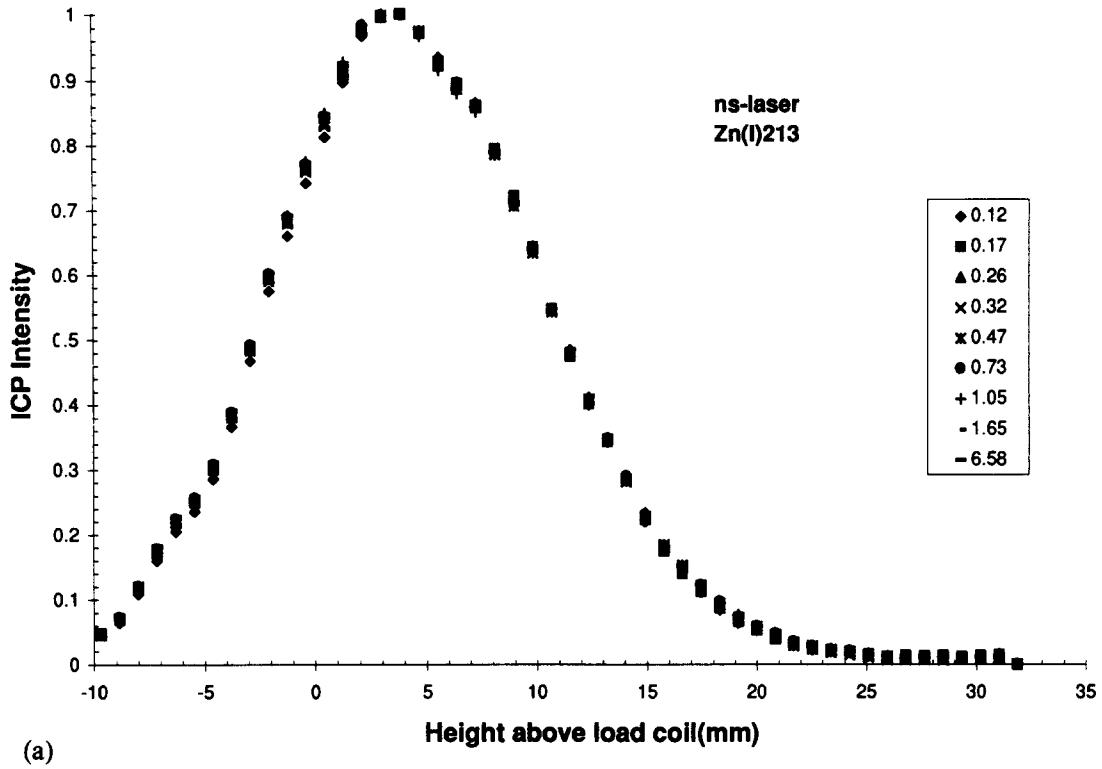

(a)

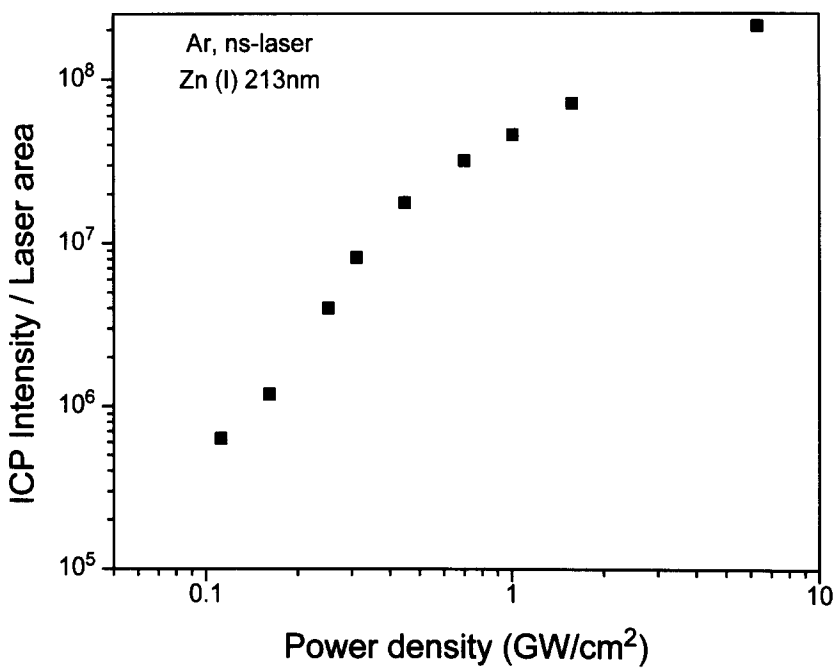

(b)

Fig. 3. Zinc emission intensity in the ICP using nanosecond laser ablation sampling of brass. (a) normalized intensity for all power densities; (b) integrated intensity versus power density.

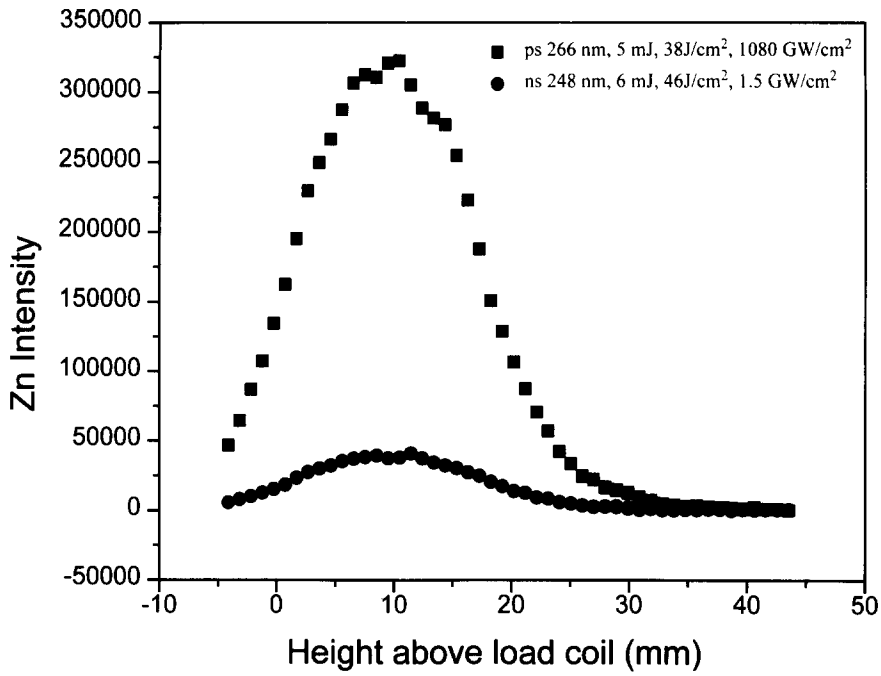

(a)

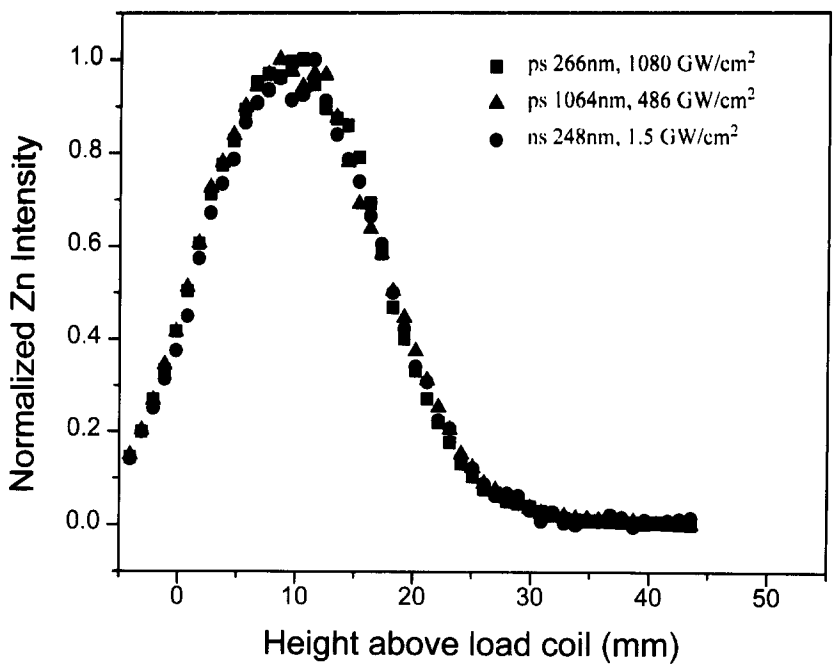

(b)

Fig. 4. Comparison of ICP emission spatial profile from Zn emission using picosecond and nanosecond laser ablation of brass. (a) emission intensity; (b) normalized emission intensity. Profiles for laser ablation sampling using both the fundamental and fourth harmonic of the N:YAG laser are included in (b).

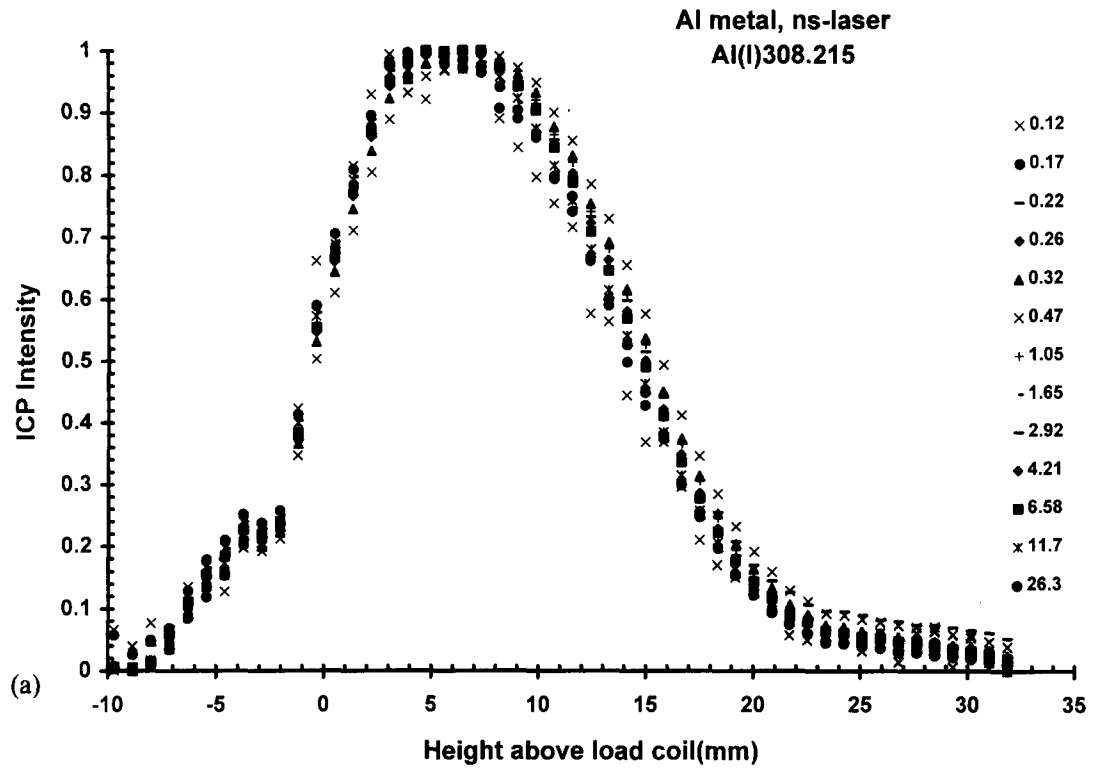
Al metal, ns-laser
Al(I)308.215
ICP Intensity
Height above load coil(mm)
0.12
0.17
0.22
0.26
0.32
0.47
1.05
1.65
2.92
4.21
6.58
11.7
26.3

(a)

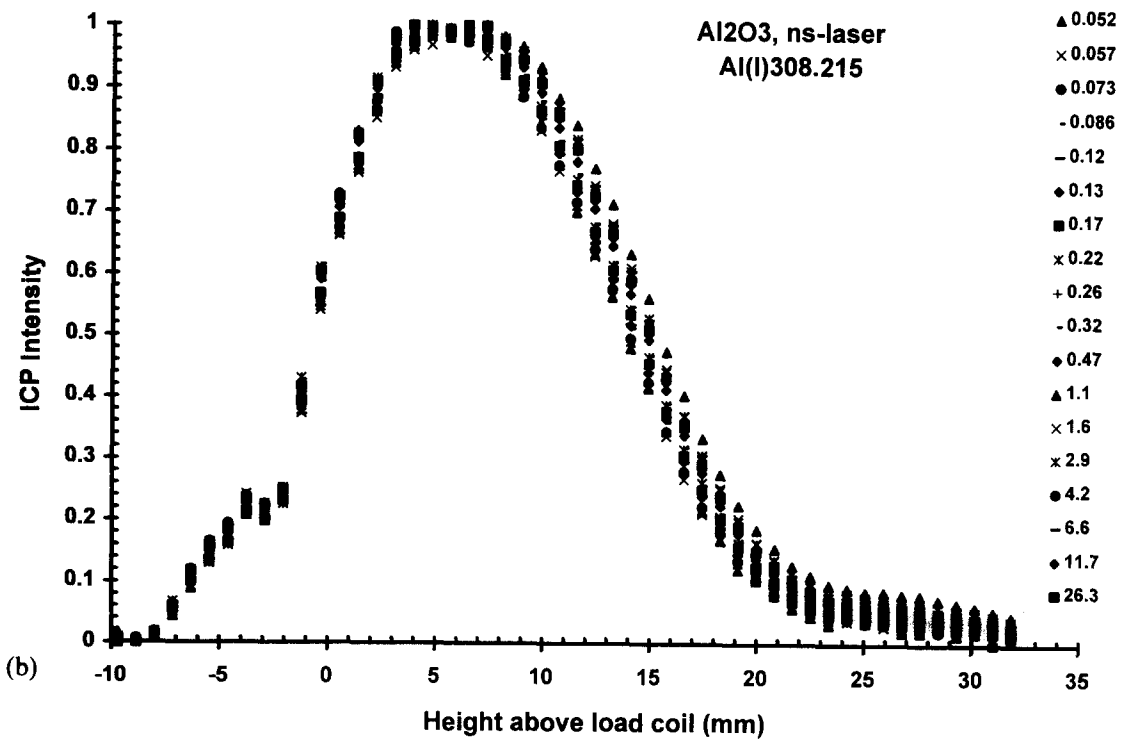
Al2O3, ns-laser
Al(I)308.215
ICP Intensity
Height above load coil (mm)
0.052
0.057
0.073
0.086
0.12
0.13
0.17
0.22
0.26
0.32
0.47
1.1
1.6
2.9
4.2
6.6
11.7
26.3

(b)

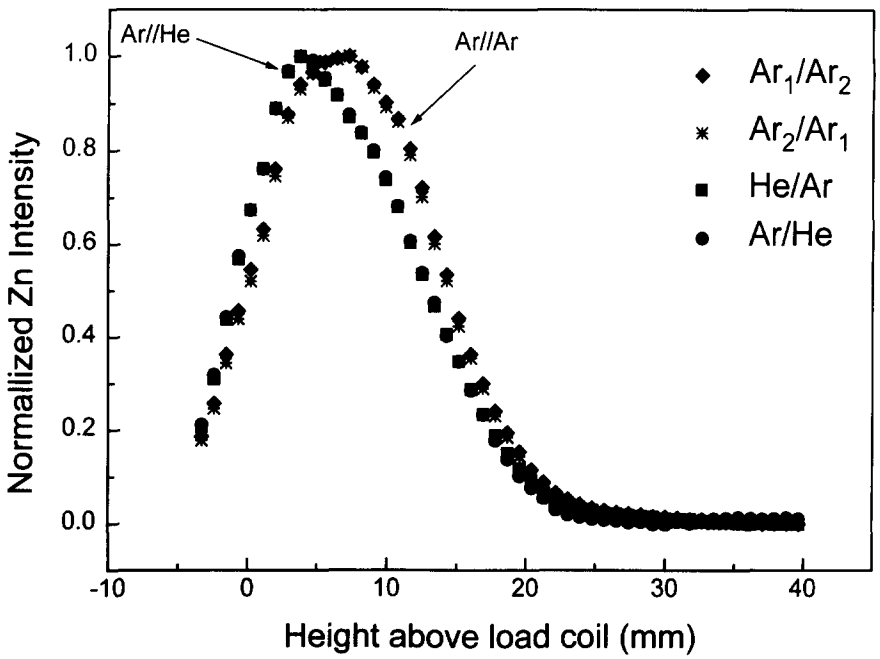

Fig. 6. Spatial Zn emission intensity profile in the ICP for picosecond Nd:YAG laser ablation of brass: Ar gas introduced into the ablation chamber and auxiliary port of the T-connector; Ar or He gas introduced into the ablation chamber or auxiliary port.

similar elements from diverse sample materials (metals versus insulators).

3.3. Spatial emission profiles versus gases

The gas environment has fundamental importance on laser ablation processes. To increase the quantity of ablated material or reduce the influence of plasma shielding, it may be beneficial to use a different gas in the ablation chamber. The coupling efficiency of laser energy to the sample may be influenced by a surface plasma [1,10,13,16,17,21]. The plasma may be responsible for shielding the laser energy from the sample and/or contributing to fractional vaporization because of its high temperature, close proximity to the sample surface, and long duration compared to the laser pulse. Plasma shielding, due to electrons and ions in the laser induced vapor, can be studied by varying the gas environment, i.e. changing the ionization potential of the ambient medium. To utilize ICP-AES for studying laser ablation processes such as plasma shielding, it is necessary to know how the spatial emission profile changes with gas composition, because the ICP temperature and excitation characteristics will change with total gas composition.

In the above studies, argon was used in the sample chamber and in the auxiliary port of the T-connector (Fig. 1). An initial experiment was to establish the error in the spatial profile when the same gas was introduced into the different inputs of the system (different mass flow controllers are used for each gas line). Four Zn spatial emission intensity profiles are shown in Fig. 6: Ar introduced into each input of the system, and He versus Ar in the chamber and auxiliary port, for picosecond laser ablation of brass. The emission spatial profiles demonstrate that slight differences in the gas flows (controllers) are not manifested in the ICP excitation characteristics (Ar// Ar), and that as expected, gas composition affects the profile (Ar//He versus Ar//Ar). Fundamental studies of laser ablation using different gases can be conducted if the total gas environment is constant, i.e.

Fig. 5. Spatial emission intensity profile in the ICP for nanosecond excimer laser ablation. (a) normalized power density curves from ablation of Al metal; (b) normalized power density curves from ablation of Al_2O_3 ceramic.

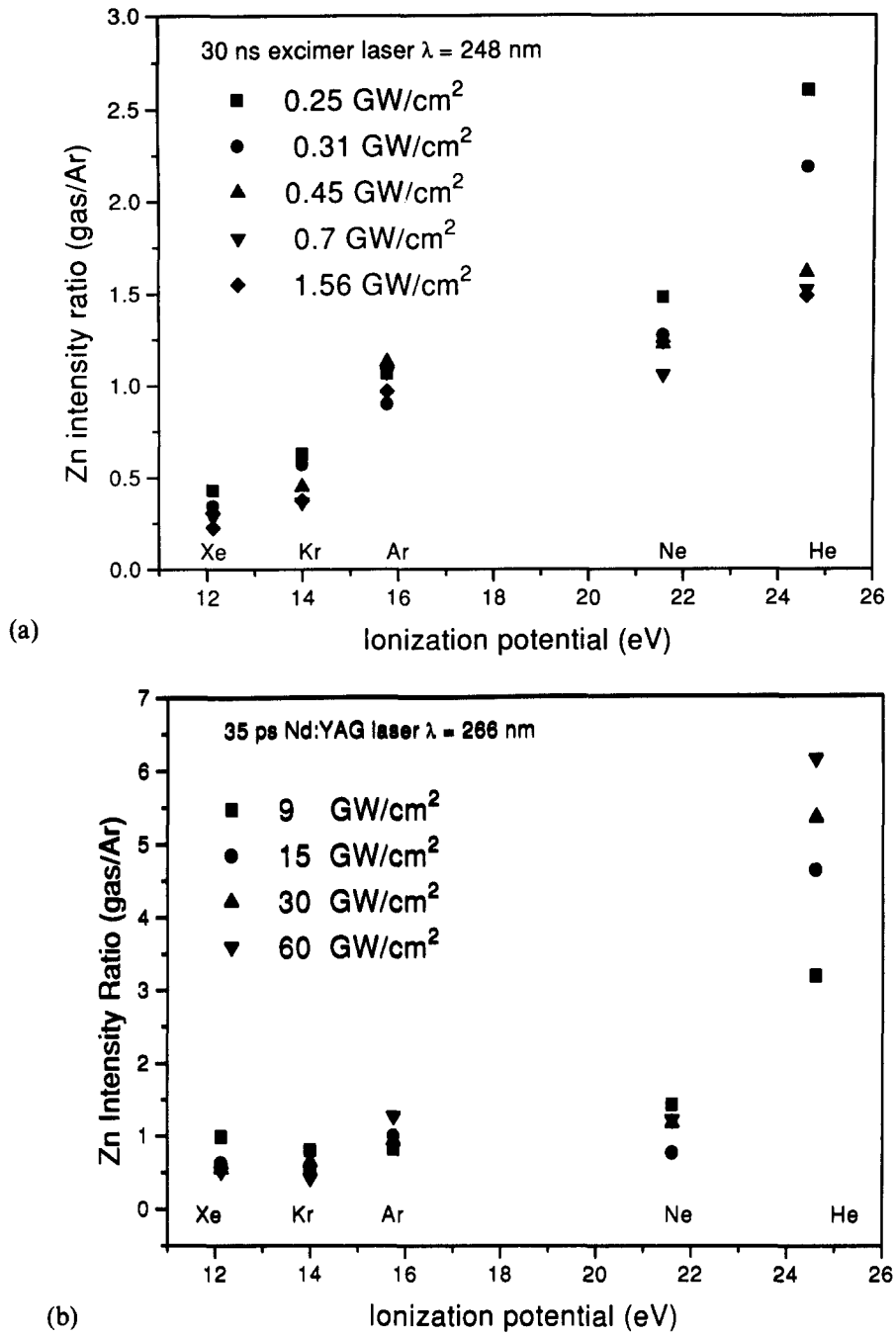

Fig. 7. Zn intensity in the ICP for laser ablation in He, Ne, Kr, and Xe versus Ar. The brass sample was ablated using UV nanosecond (a) and picosecond (b) laser pulses at several laser power densities.

constant spatial emission profile. Previously, we showed that laser ablation using He in the sample chamber increased ICP spectral emission intensity compared to an ICP with the same mixture but with Ar in the chamber [10]. Combinations of Ar with He, Ne, Kr, Xe, and N_2 have been performed by alternating their path through the chamber or directly into the auxiliary connector [38]. The ratios of ICP intensity

for ablation in a specific gas to that in Ar, for nanosecond and picosecond pulses, are shown in Fig. 7a and Fig. 7b, respectively. A complete discussion of these gas effects is beyond the scope of this manuscript and will be discussed in a subsequent paper. The noble gases in the sample chamber either enhance or decrease the quantity of mass ablated (emission intensity in the ICP), with the degree of influence dependent on the laser power density. In all cases, the ICP spatial emission profile was measured to be constant, indicating that these intensity data accurately represent changes in the laser ablation processes.

4. Conclusion

This work demonstrated that the spatial emission intensity profile in the ICP for a particular element does not change under diverse laser conditions (power density, pulse duration, and wavelength), and when the element originates from diverse sample targets. Therefore, accuracy can be maintained as the power density or sample material changes. The roll-off in mass ablation versus power density is not a manifestation of changing spatial emission profile; it remained constant throughout the roll-off power density region for both nanosecond and picosecond laser ablation sampling. Complementary experiments that do not rely on transport or emission show roll-off with power density, with the deflection point occurring at the same power density as measured by the ICP [39,40]. Preferential vaporization which is as a function of power density, also is not a manifestation of a shifting spatial profile; the profile remains constant through the power density range in which the mass ablation rate ratio changes. It is possible that the range of power densities used in these studies did not change the particle size distribution by a significant amount to affect vaporization and excitation in the ICP; the temperature and excitation characteristics of the ICP appear to dominate the emission spatial profile for the majority of particles reaching the plasma. The laser parameters studied in this work represent diverse conditions that probably would not exist in conventional analytical laser ablation sampling systems, guaranteeing that under less severe conditions, the spatial emission profile will remain constant for fixed ICP operating conditions. Finally, fundamental studies of laser ablation processes based on gas environments can be performed using ICP-AES as long as the total gas composition to the ICP remains constant.

Acknowledgements

The authors are grateful for experimental assistance from Wing-Tat Chan and Amy Leung. This work was supported by the US Department of Energy, Office of Basic Energy Sciences, Division of Chemical Sciences, Processes and Techniques Branch, under contract number DE-AC03-76SF00098.

References

[1] R. Russo, Appl. Spectrosc. A, 49 (1995) 14.
[2] S.A. Darke and J.F. Tyson, J. Anal. Atom. Spectrom., 8 (1993) 145.
[3] L. Moenke-Blankenburg, Spectrochim. Acta Rev., 15 (1993) 1.
[4] R.D. Evans, P.M. Outridge and P. Richner, J. Anal. Atom. Spectrosc., 9 (1994) 985–989.
[5] A.J. Walder, I.D. Abell, I. Platzner and P.A. Freedman, Spectrochim. Acta, Part B, 48 (1993) 397–402.
[6] L. Moenke-Blankenburg, T. Schumann, D. Gunther, H.M. Kuss and M. Paul, J. Anal. Atom. Spectrosc., 7 (1992) 251–254.
[7] N. Furuta, Appl. Spectrosc., 45 (1991) 1372–1376.
[8] Z.W. Hwang, Y.Y. Teng and J. Sneddon, Microchem. J., 43 (1991) 42–45.
[9] W.T. Chan and R.E. Russo, Spectrochim. Acta, Part B, 46 (1991) 1471.
[10] X.L. Mao, W.-T. Chan, M.A. Shannon and R.E. Russo, J. Appl. Phys., 74 (1993) 4915.
[11] W.T. Chan, X.L. Mao and R.E. Russo, Appl. Spectrosc., 46 (1992) 1025.
[12] A. Fernández, X.L. Mao, W.T. Chan, M.A. Shannon and R.E. Russo, Anal. Chem., 67 (1995) 2444–2450.
[13] M.A. Shannon, X.L. Mao, A. Fernández, W.-T. Chan, and R.E. Russo, Anal. Chem., 67 (1995) 4522–4529.
[14] R.E. Russo, X.L. Mao, W.T. Chan, M.F. Bryant and W.F. Kinard, J. Anal. Atom. Spectrom., 10 (1995) 295.
[15] M. von Allmen, in Laser-Beam Interactions with Materials — Physical Principles and Applications, Springer-Verlag, New York, 1987.
[16] N. Bloembergen, in S.D. Ferris, H.J. Leamy and J.M. Poate (Eds.), Laser–Solid Interaction and Laser Processing, American Institute of Physics, New York, 1979.
[17] J.F. Ready, in Effect of High-Power Laser Radiation, Academic Press, New York, 1971.
[18] P. Arrowsmith and S.K. Hughes, Appl. Spectrosc., 42 (1988) 1231.

[19] M. Thompson, S. Chenery and L. Brett, J. Anal. Atom. Spectrosc., 5 (1990) 49–55.
[20] E.F. Cromwell and P. Arrowsmith, Appl. Spectrosc., 49 (1995) 1652–1660.
[21] T. Mochizuki, A. Sakashita, T. Tsuji, H. Iwata, Y. Ishibashi and N. Gunji, Anal. Sci., 7 (1991) 479–481.
[22] A.A. van Heuzen, Spectrochim. Acta, Part B, 46 (1991) 1803–1817.
[23] A.A. van Heuzen and J.B.W. Morsink, Spectrochim. Acta, Part B, 46 (1991) 1819–1828.
[24] L. Ebdon, M.E. Foulkes and S. Hill, J. Anal. Atom. Spectrom., 5 (1990) 67.
[25] T. Mochizuki, A. Sakashita, H. Iwata, Y. Ishibashi and N. Gunji, Anal. Sci., 5 (1989) 311.
[26] K.E. Jarvis and J.G. Williams, Chem. Geol., 77 (1989) 53.
[27] J.G. Williams, A.L. Gray, P. Norman and L. Ebdon, J. Anal. Atom. Spectrom., 2 (1987) 469.
[28] L. Halicz and I.B. Brenner, Spectrochim. Acta, Part B, 42 (1987) 207.
[29] M.W. Blades and G. Horlick, Spectrochim. Acta, Part B, 36 (1981) 861.
[30] X.L. Mao and R.E. Russo, J. Anal. Atom. Spectrom., submitted.
[31] R.E. Russo, Direct Solid Introduction to the ICP using a Repetitively Pulsed Nd:YAG Laser, Federation of Analytical Chemistry and Spectroscopy Societies meeting, Philadelphia, PA, September 1984.
[32] P. Arrowsmith, Anal. Chem., 59 (1987) 1437.
[33] X.L. Mao, M.A. Shannon, A.J. Fernandez and R.E. Russo, Appl. Spectrosc., 49 (1995) 1054.
[34] X.R. Liu and G. Horlick, Spectrochim. Acta, Part B, 50 (1994) 537–548.
[35] T.V. Venkatesan, in J.C. Miller (Ed.), Laser Ablation: Principles and Applications, Springer Series in Material Science 28, Springer Verlag, New York, 1994.
[36] D.B. Chrisey and G.K. Hubler (Eds.), Pulsed Laser Deposition of Thin Films, Wiley, New York, 1994.
[37] C. Geertsen, A. Briand, F. Chartier, J.L. Lacour, P. Mauchien, S. Sjostrom and J.M. Mennet, J. Anal. Atom. Spectrosc., 9 (1994) 17–22.
[38] R.E. Russo, X.L. Mao, M.A. Shannon and M. Caetano, Appl. Surface Sci., 96 (1996) 144–148.
[39] M.A. Shannon and R.E. Russo, Appl. Phys. Lett., 67 (1995) 3227–3229.
[40] M.A. Shannon, B. Rubinsky and R.E. Russo, J. Appl. Phys., accepted for publication.